Supplementary Information for

Crystal Structure and Electronic Properties of 2-Amino-2-Methyl-1-Propanol (AMP) Carbamate

Eunhee Jo,† Young Ho Jhon,† Sang Beom Choi,† Jae-Gu Shim,‡ Jun-Han Kim,‡ Ji Hyun Lee,‡ In-Young Lee,‡ Kyung-Ryong Jang ‡ and Jaheon Kim*,†

†Department of Chemistry, Soongsil University, Seoul 156-743, Korea; ‡Global Environment Research Group, Environment & Structure Laboratory, Korea Electric Power Research Institute, Daejeon 305–380, Korea

E-mail: jaheon@ssu.ac.kr

Preparation of the AMP-carbamate salt (1): $[HO(CH_2)C(CH_3)_2NH_3][HO(CH_2)C(CH_3)_2NHCOO]$

AMP (2-amino-2-methyl-propanol) was purchased from the Aldrich Chemical Co. and used without further purification. AMP (5.0 mL, 52.2 mmol) was put in a round bottomed flask which was fitted with a funnel filled with a drying agent. After exposure to air for 5 days, white precipitates formed (see the picture below). The solid was washed with hexanes, and dried in vacuum (1.04g, 4.68 mmol, 17.9%). ^{1}H-NMR (400MHz, D_2O, *δ,* ppm): 3.49(s, 2H, C*H*), 1.22(s, 6H, C*H*$_3$); ^{13}C-NMR(100MHz, D_2O, *δ,* ppm): 166.23(HCO_3^-), 70.83(CH_2), 56.23(NH*C*$(CH_3)_2CH_2$, NH_3^+*C*$(CH_3)_2CH_2$), 25.44(CH_3); ^{1}H-NMR (400MHz, DMSO, *δ,* ppm): 4.57(s,O*H*,N*H*$_3^+$), 3.07(s, 2H, C*H*), 0.92(s, 6H, C*H*$_3$); ^{13}C-NMR(100MHz, DMSO, *δ,* ppm): 160.23(HCO_3^-), 70.28(CH_2), 52.53(NH*C*$(CH_3)_2CH_2$), 51.39 (NH_3^+*C*$(CH_3)_2CH_2$), 25.71(CH_3), 24.49(CH_3). Element analysis, calculated for $C_9H_{22}N_2O_4$: C 48.63, H 9.98, N 12.60 % ; found: C 47.89, H 10.35, N 12.21%; FT-IR (KBr, cm^{-1}): 3318(w), 3231(w), 2974(w), 2729(w), 2605(w), 2541(w), 2163(s), 1648(w), 1581(w), 1500(w), 1359(w), 1310(w), 1270(w), 1175(w), 1087(w), 1059(s), 980(w), 826(w), 767(w), 695(w), 558(w); mp. : 88-89 °C.

IR spectra of AMP and AMP-carbamate salt

(a)

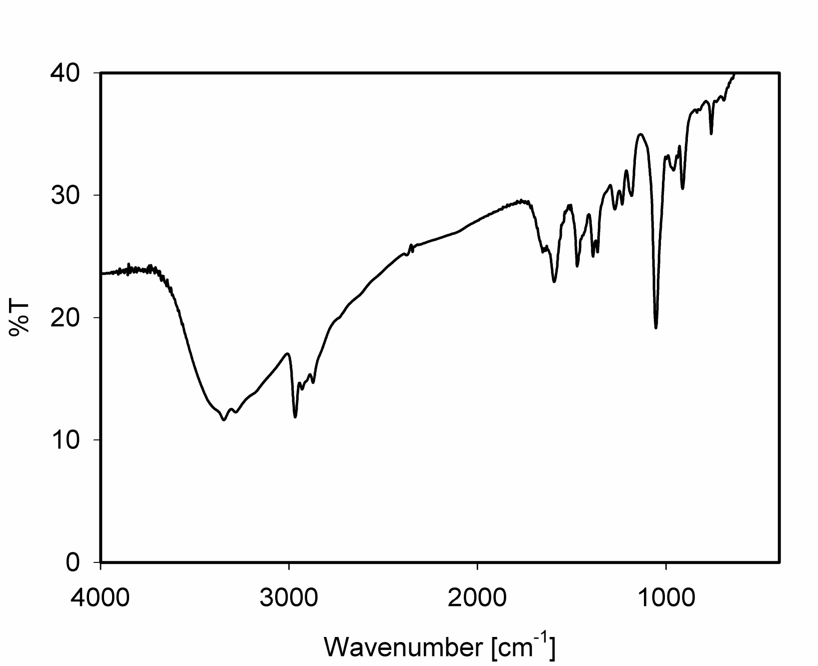

(b)

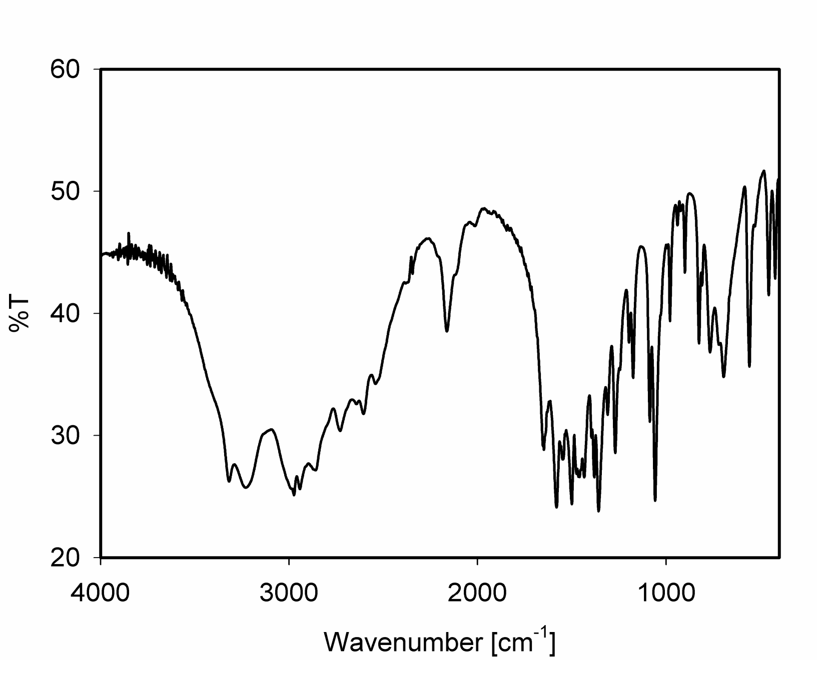

Figure S1. FT-IR spectra of (a) AMP and (b) **1**.

^{1}H-NMR spectra of AMP and AMP-carbamate salt in D_2O

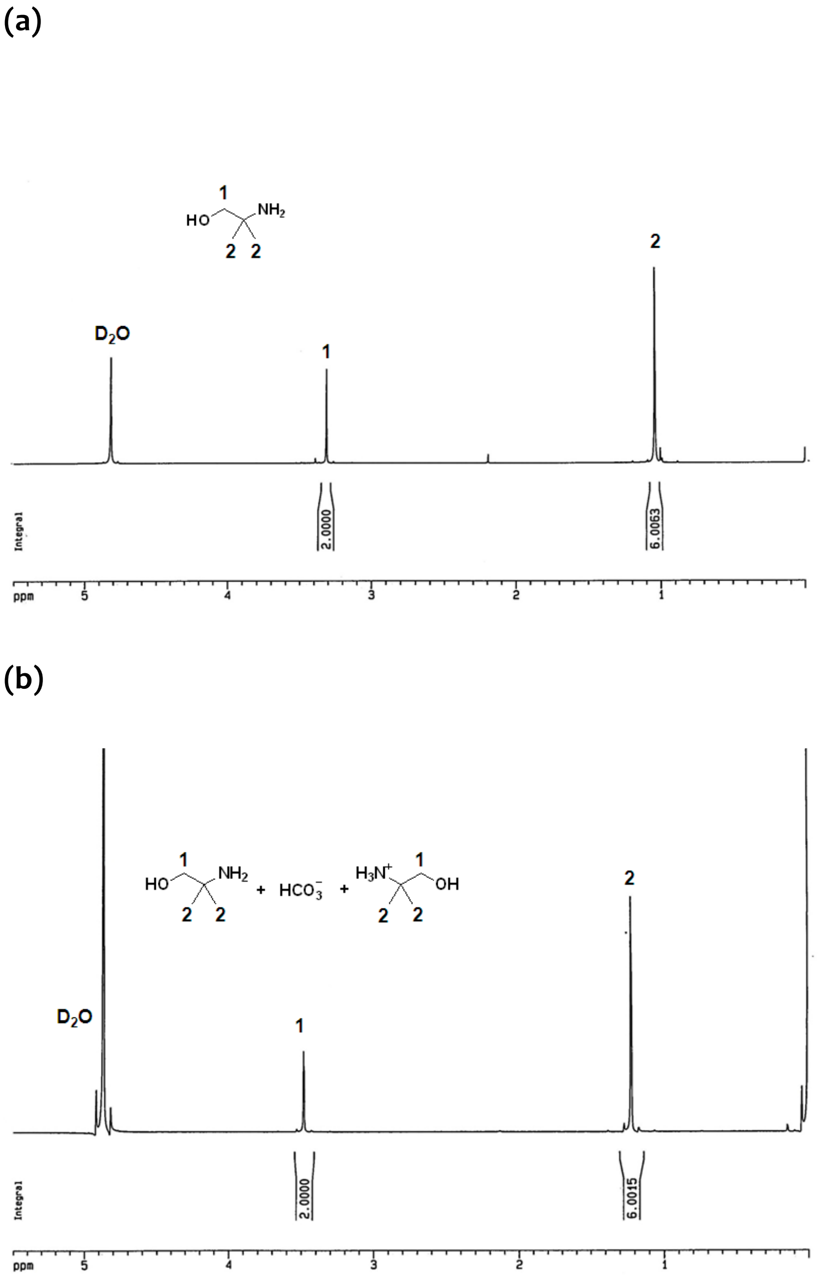

Figure S2. ^{1}H-NMR (400 MHz, D_2O) spectra of (a) AMP and (b) **1**. AMP carbamate is hydrolyzed into bicarbonate and protonated-AMP.

^{1}H-NMR spectra of AMP and AMP-carbamate salt in DMSO

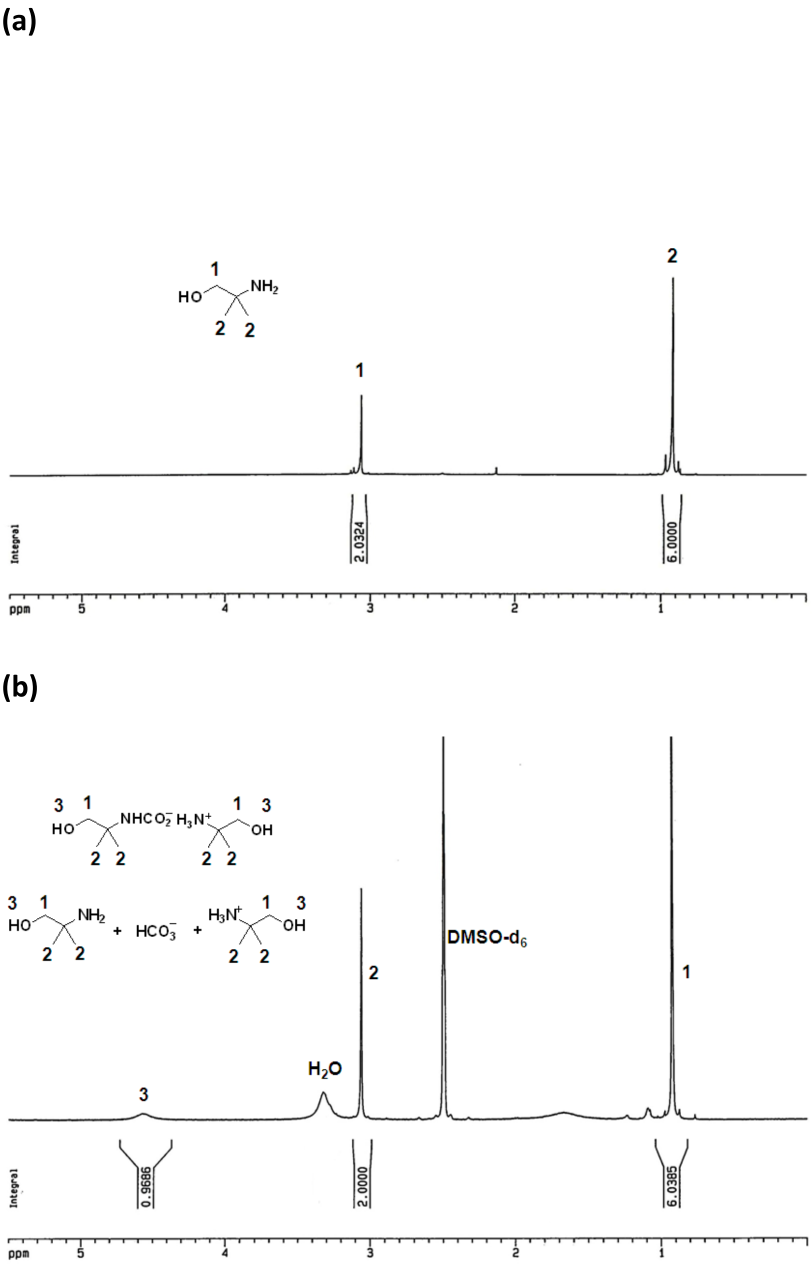

Figure S3. ^{1}H-NMR (400 MHz, DMSO) spectra of (a) AMP and (b) **1**. AMP carbamate is partially hydrolyzed into bicarbonate and protonated-AMP.

^{13}C-NMR spectra of AMP and AMP-carbamate salt in D_2O

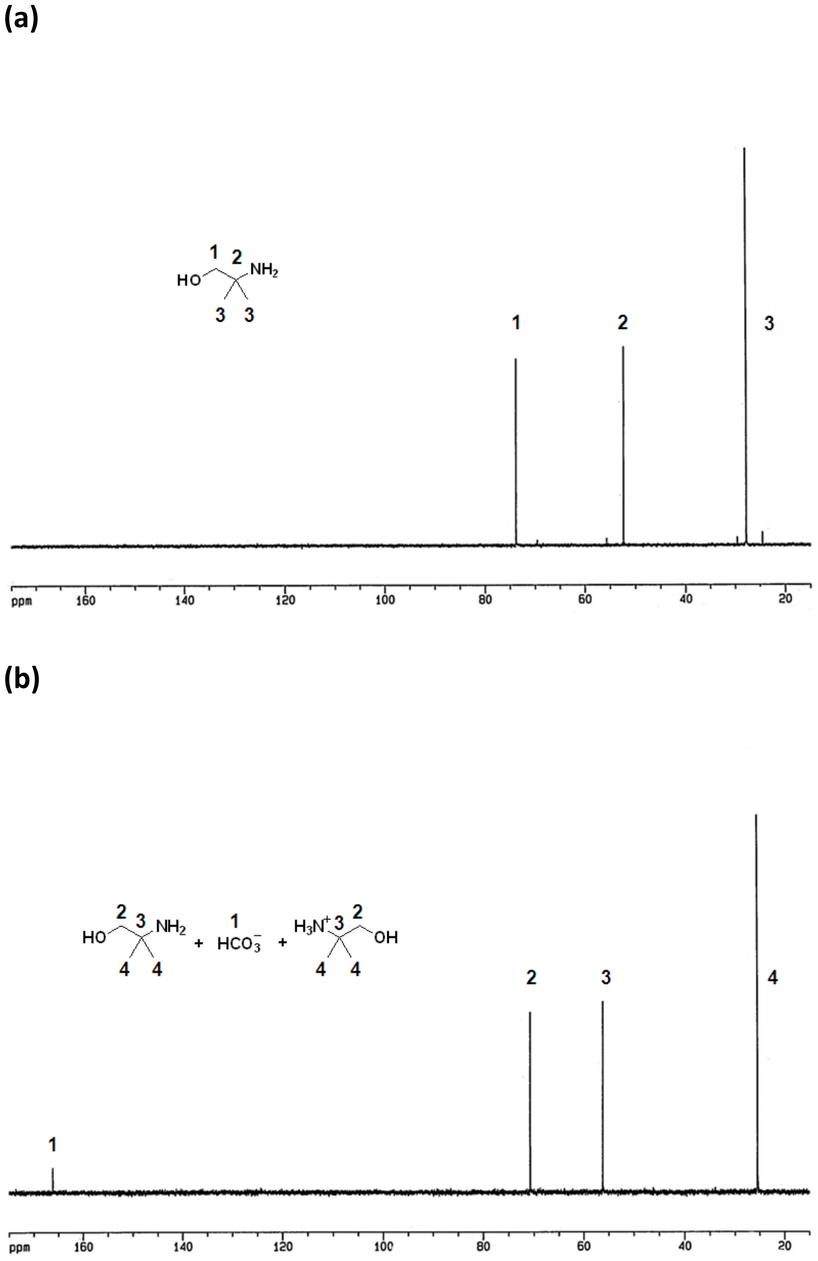

Figure S4. ^{13}C-NMR (100 MHz, D_2O) spectra of (a) AMP and (b) **1**. AMP carbamate is hydrolyzed into bicarbonate and protonated-AMP.

^{13}C-NMR spectra of AMP and AMP-carbamate salt in DMSO

(a)

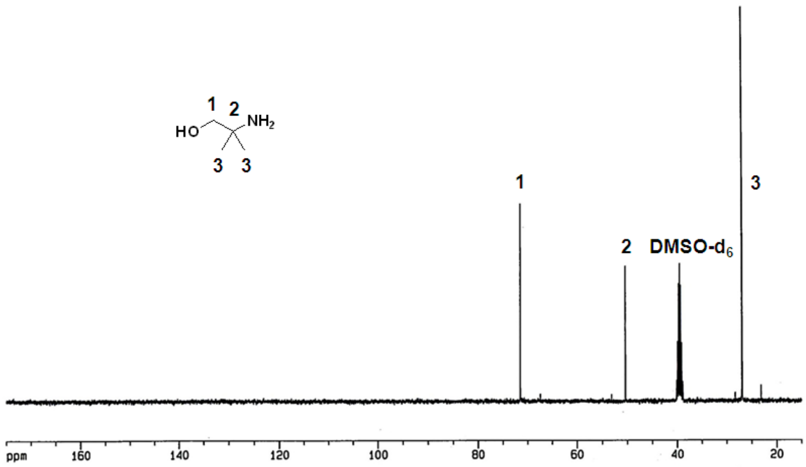

(b)

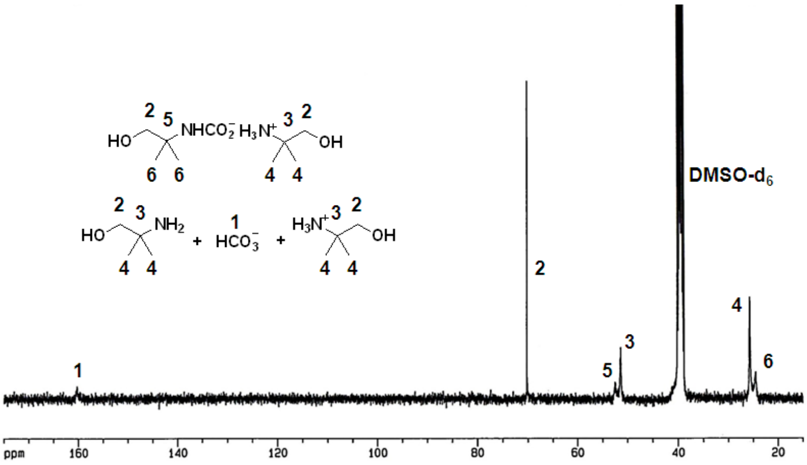

Figure S5. ^{13}C-NMR (100 MHz, DMSO) spectra of (a) AMP and (b) **1**. AMP carbamate is partially hydrolyzed into bicarbonate and protonated-AMP.

^{13}C-NMR spectra of AMP-carbamate salt in DMSO after exposure to air

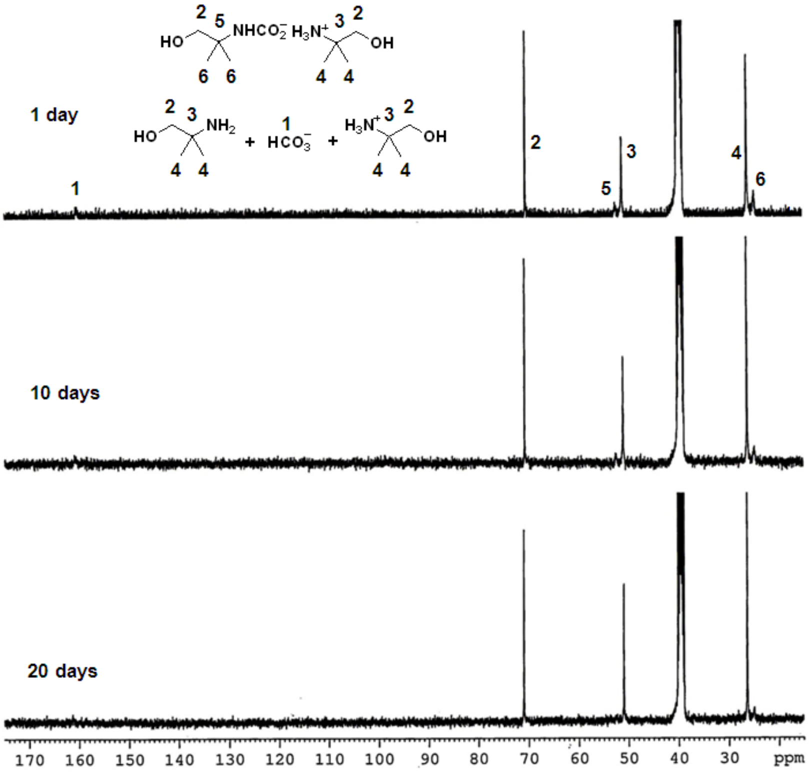

Figure S6. ^{13}C-NMR (100 MHz, DMSO) spectra of **1**. AMP carbamate is partially hydrolyzed into bicarbonate and protonated-AMP.

Thermal analyses of AMP and 1: TGA

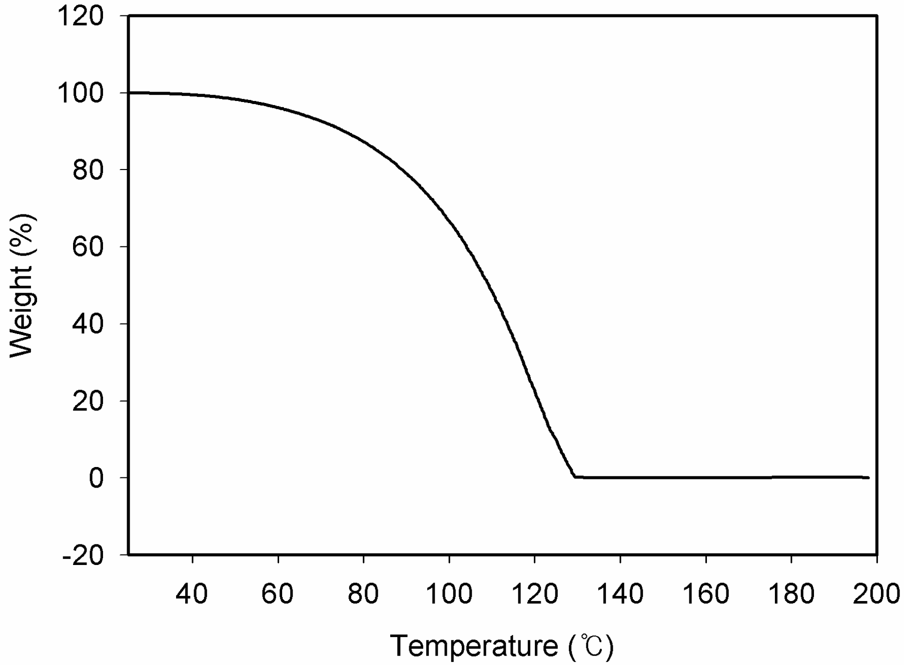

(a)

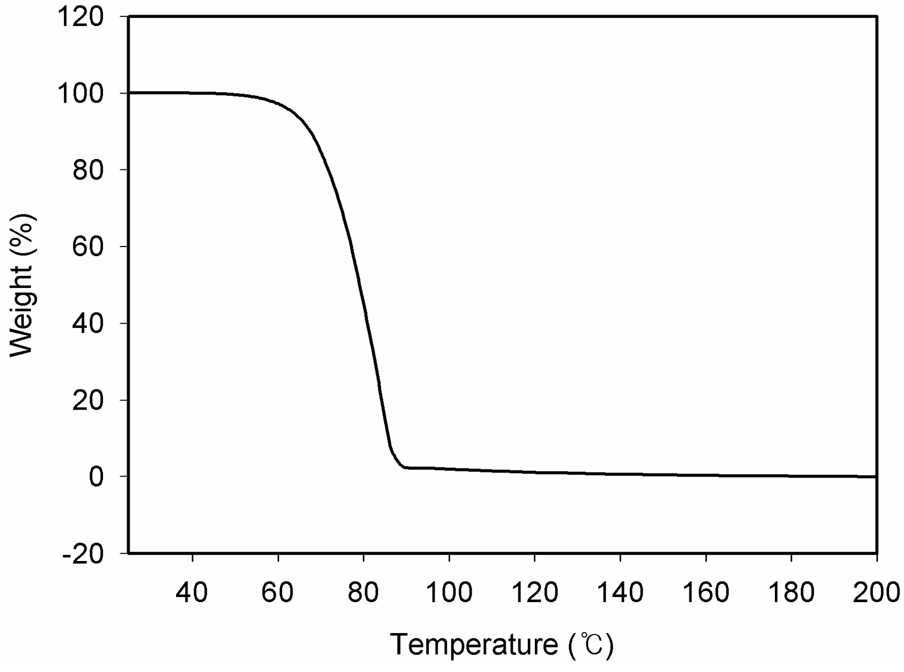

(b)

Figure S7. Thermogravimetric analysis (TGA) traces of (a) AMP and (b) **1**. Temperature was increased at 10 °C/min under nitrogen atmosphere.

Thermal analyses of AMP-carbamate salt: DSC

The DSC data were collected from 0 to 19.2275 min or 24.3189 to 214.5466 °C. The heat flow in the range of 4.8247–10.0542 min (69.58–122.22 °C) was integrated to give -73.60 mW·min. Considering the sample weight (0.00496 g) and molar weight (222.29 g) of 1, the endothermic heat flow was converted to -47.22 kcal/mol.

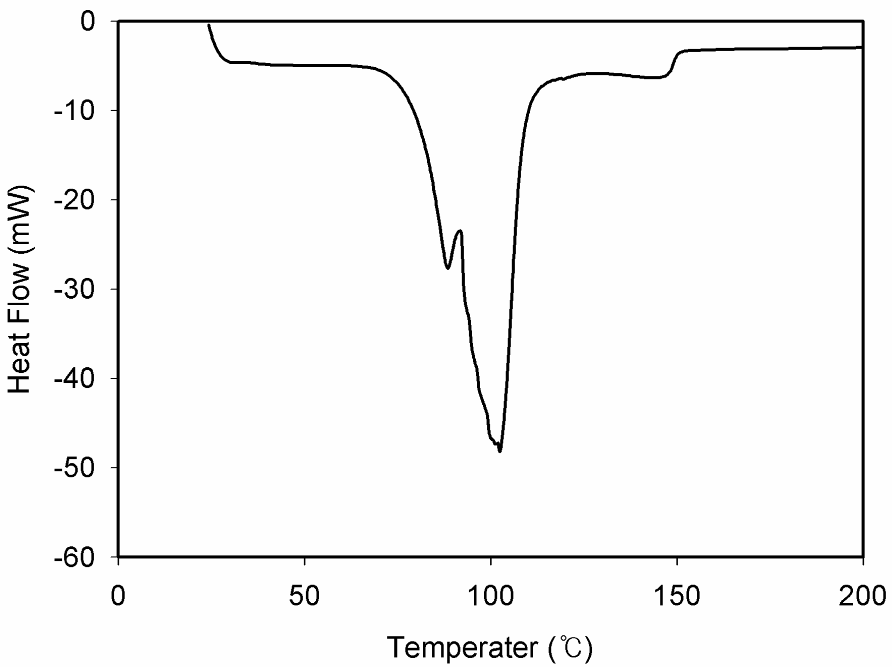

Figure S8. Differential scanning calorimetry (DSC) trace of **1**. Temperature was increased at 10 °C/min under nitrogen atmosphere.

Single crystal X-ray diffraction analysis of AMP-carbamate salt

Crystallization of 1. Suitable crystals for the single crystal X-ray diffraction analysis were obtained by vapor diffusion methods. AMP-carbamate solid (20 mg, 0.09 mmol) was dissolved in DMF(0.2 mL) in a small vial (4 mL) that was put in a large vial (20mL) containing 1.0 mL of hexane. When the large vial was capped tightly and standing at ambient temperature for 4 days, colorless block crystals were obtained (2.4 mg, 0.01 mmol, 12 %).

Single crystal X-ray diffraction analysis. The diffraction data set from a clear block crystal was collected at 173 K on a Bruker APEX-II CCD diffractometer with MoKα radiation (λ = 0.71037 Å). Bruker APEX2 program was used for data collection, and SAINT was used for cell refinement, and reduction. Absorption correction was applied using SADABS. Crystal structure was solved using SHELX-TL software package with a monoclinic space group, $P2_1/n$ (No. 14). An initial structure was obtained by direct methods using XS, and improved by subsequent refinements using XL. Non-hydrogen atoms were refined anisotropically. All hydrogen atoms were found in the difference Fourier maps, and both their positions and thermal parameters were refined without any restraints. The final refinement process converged to R1 = 0.0389, wR2 = 0.0972 ($I > 2\sigma(I)$). Crystal and refinement data are given in Table S1. Bond distances and angles of hydrogen bonds are listed in Table S2. ORTEP diagram of the asymmetric unit is displayed in Figure S9 and the packing diagram is shown in Figure S10.

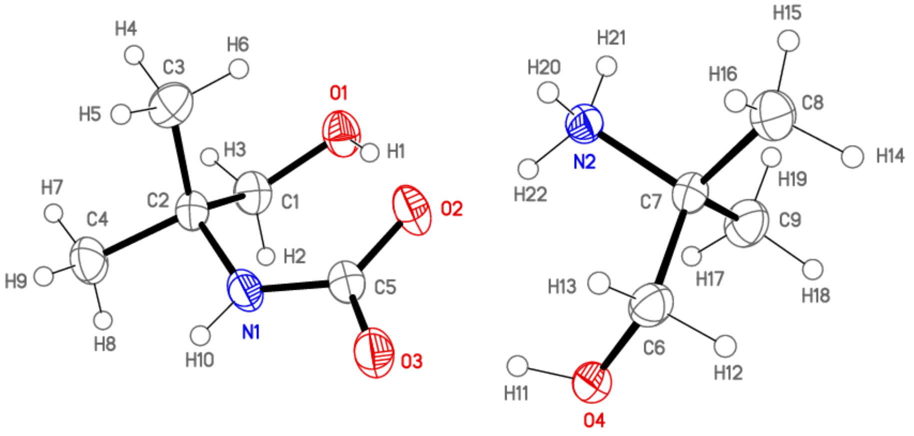

Figure S9. The asymmetric unit of **1** is drawn with 50 % thermal ellipsoids by ORTEP.

Table S1. Crystal data and structure refinement for **1**.

Empirical formula	$C_9 H_{22} N_2 O_4$	
Formula weight	222.29	
Temperature	173(2) K	
Wavelength	0.71073 Å	
Crystal system	monoclinic	
Space group	$P2_1/n$	
Unit cell dimensions	a = 6.0537(3) Å	α= 90°.
	b = 9.9108(6) Å	β= 98.102(4)°.
	c = 20.4773(12) Å	γ = 90°.
Volume	1216.31(12) $Å^3$	
Z	4	
Density (calculated)	1.214 g/cm^3	
Absorption coefficient	0.094 mm^{-1}	
F(000)	488	
Crystal size	0.33 x 0.28 x 0.27 mm^3	
Theta range for data collection	2.01 to 27.55°.	
Index ranges	-7<=h<=7, -12<=k<=12, -26<=l<=26	
Reflections collected	11047	
Independent reflections	2791 [R(int) = 0.0312]	
Completeness to theta = 27.55°	99.7 %	
Absorption correction	Empirical	
Refinement method	Full-matrix least-squares on F^2	
Data / restraints / parameters	2791 / 0 / 224	
Goodness-of-fit on F^2	1.046	
Final R indices [I >2σ(I)]	R1 = 0.0389, wR2 = 0.0972	
R indices (all data)	R1 = 0.0491, wR2 = 0.1027	
Largest diff. peak and hole	0.301 and -0.193 e.$Å^{-3}$	

Table S2. Hydrogen bonds for **1** [Å and °].

D□H...A	d(D□H)	d(H...A)	d(D...A)	∠(D□H...A)
O(1) □H(1)...O(2)	0.85(2)	1.71(2)	2.5493(14)	169.4(19)
N(1) □H(10)...O(3)$^{\#1}$	0.874(18)	2.087(19)	2.9571(15)	173.4(16)
O(4) □H(11)...O(3)	0.88(2)	1.70(2)	2.5743(14)	172(2)
N(2) □H(20)...O(1)$^{\#2}$	0.929(17)	1.879(18)	2.8054(15)	174.3(15)
N(2) □H(21)...O(4)$^{\#3}$	0.893(19)	1.880(19)	2.7679(15)	172.3(16)
N(2) □H(22)...O(2)	0.968(17)	1.786(17)	2.7271(15)	163.2(15)

Symmetry transformations used to generate equivalent atoms:

#1 -x+1,-y+1,-z+1 #2 x-1,y,z #3 -x+1/2,y-1/2,-z+1/2

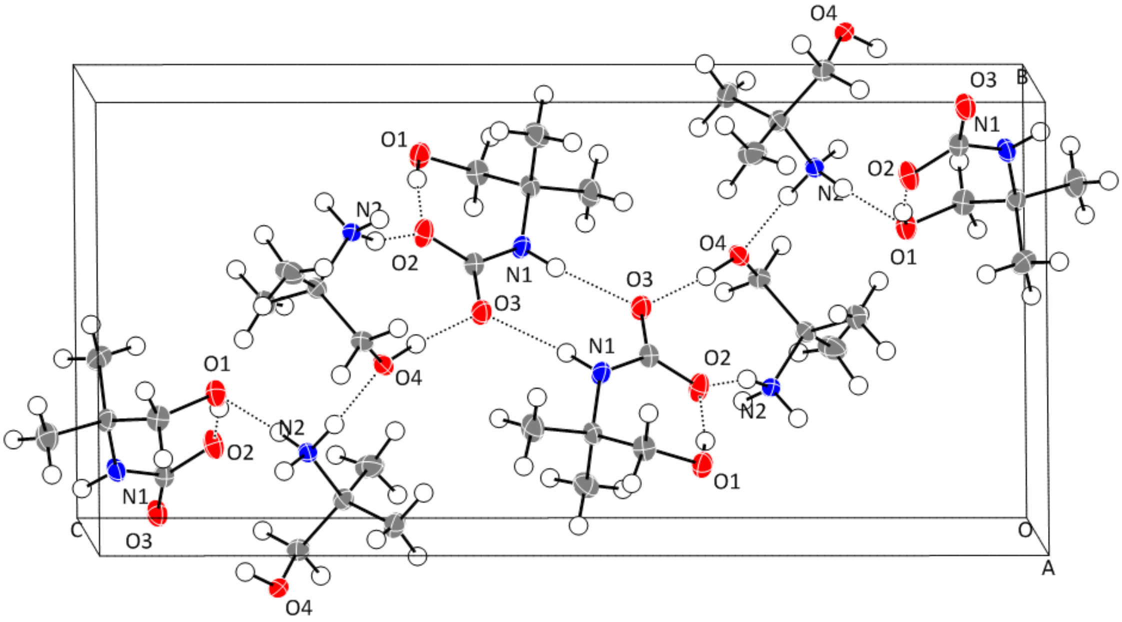

Figure S10. The packing diagram of **1** is shown with hydrogen bonds.

DFT-optimized structures for AMP carbamate

The AMP- and MEA- carbamate molecular structures are optimized using DFT calculation (B3LYP/6-31+G(d,,p)), with the crystal structure as initial guess. Here the initial structure of MEA-carbamate is the AMP-carbamate crystal structure where two methyl groups on C_α atom are replaced with H atoms.

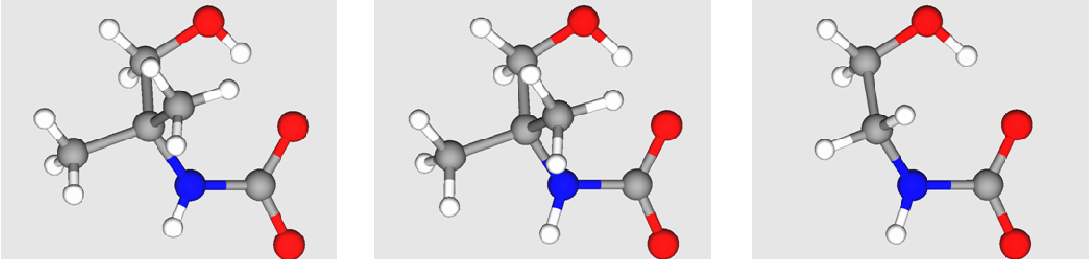

(a) (b) (c)

Figure S11. (a) Crystal and (b) DFT-optimized AMP carbamates, and (c) DFT-optimized MEA carbamate structures are displayed with ball-and-stick models (B3LYP/6-311++G(d,p)).

Table S3. Summary of the geometric parameters for AMP- and MEA-carbamates. See Figures S8, S13 for the atomic labels.

Geometry	AMP carbamates			MEA carbamate	
	Crystal Structure	B3LYP/ 6-311++G(d,p)	MP2/ 6-311++G(d,p)	B3LYP/ 6-311++G(d,p)	MP2/ 6-311++G(d,p)
		Gas phase	PCM solvation	Gas phase	PCM solvation
∠(O1–C1–C2–N1), °	74.30	76.821	76.677	75.521	73.126
d(N1–C5) for AMP-carbamate, *d*(N1-C3) for MEA-carbamte, Å	1.361	1.445	1.400	1.444	1.396
Sum of the bond angles around N1, °	355.54	347.122	350.880	345.696	349.652
□(C2–C1–O1–H1), °	39.35	43.986	42.662	31.987	26.317
∠(O1–H1...O2), °	169.49	164.444	165.951	165.659	167.571
d(H1...O2), Å	1.71	1.608	1.642	1.650	1.691
d(O1...O2), Å	2.549	2.589	2.611	2.631	2.661

Dissociation of N-C bond of AMP- and MEA-carbamates

The dissociation energies of N–C bond in AMP- and MEA- carbamates have been computed using B3LYP/6-311++G(d,p) DFT methods by calculating enthalpy changes at 298K:

$$E(\text{amine}\,\bullet) + E(\text{COO}^{-}\bullet) - E(\text{amine\_carbamate})$$

The calculated dissociation energies of N–C bond of AMP- and MEA-carbamates were 81.920 and 82.934 kcal/mol, respectively

Natural bond orbital (NBO) and Second order perturbation Analysis: donor – acceptor interaction

Natural bond orbital analysis is performed to investigate interactions of orbitals using B3LYP/6-311++G(3df,3pd) in PCM salvation model. The interaction between a filled donor orbital (*i*) and vacant acceptor orbital (*j*) can be calculated using second order perturbation analysis. The stabilization energy E(2) associated with delocalization is estimated as

$$E(2) = \Delta E_{ij} = q_i \frac{F(i,j)^2}{\varepsilon_j - \varepsilon_i}$$

Here, q_i is the donor orbital occupancy, ε_i and ε_j are diagonal elements (orbital energies) and F(i,j) is the off-diagonal NBO Fock matrix element.

Table S4. Second order perturbation analysis for the interaction between electron donor and acceptor orbitals in NBO basis for AMP-carbamate: BD* = antibonding orbital.

donor NBO (*i*)	acceptor NBO (*j*)	E(2)[a] (kcal/mol)	ε_j - ε_i (a.u.)	F(i,j) (a.u.)
LP(1) N1	BD^*(1) C5-O3	24.87	0.38.	0.092
	BD^*(1) C2-C3	8.365	0.6410	0.0680
	BD^*(1) C1-C2	2.79	0.63	0.039
	BD^*(1) C3-H4	0.69	0.69	0.020

[a] Hyperconjugative interaction energy.

Table S5. Second order perturbation analysis for the interaction between electron donor and acceptor orbitals in NBO basis for MEA-carbamate.

donor NBO (*i*)’	acceptor NBO (*j*)’	E(2)[a] (kcal/mol)	ε_j - ε_i (a.u.)	F(i,j) (a.u.)
LP(1) N1	BD^*(1) C3-O3	24.30	0.39	0.091
	BD^*(1) C2-H4	6.85	0.67	0.063
	BD^*(1) C1-C2	3.63	0.65	0.045

[a] Hyperconjugative interaction energy.

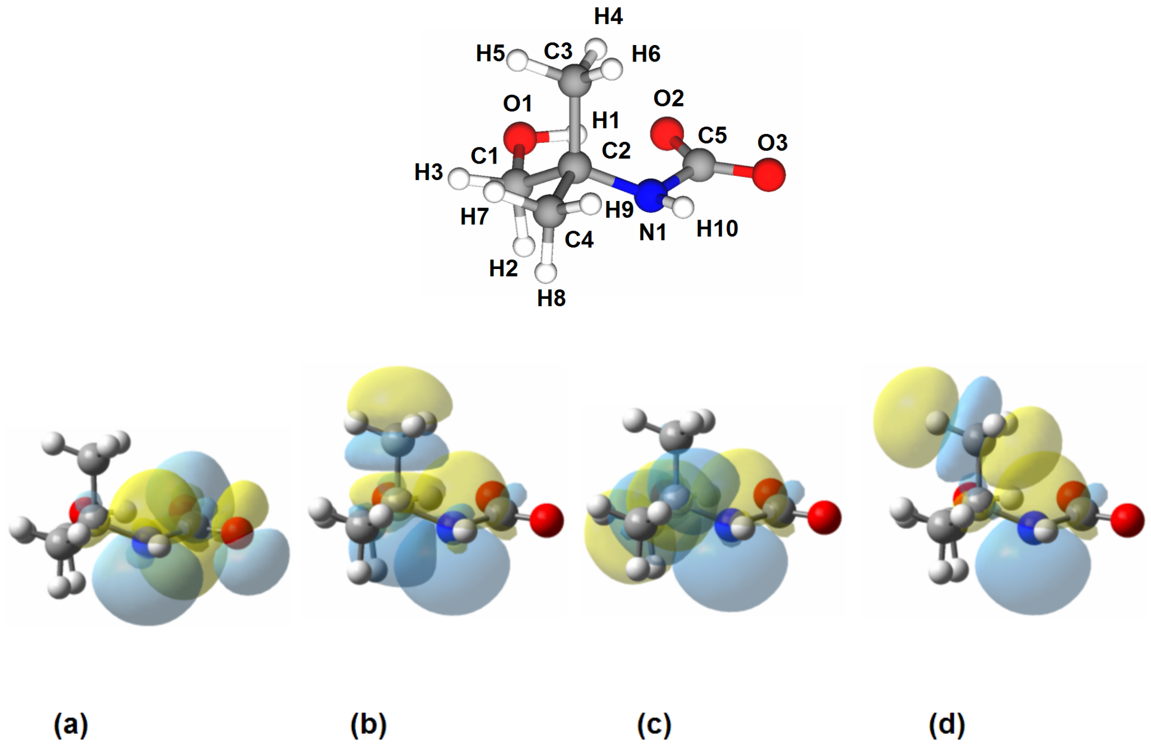

Figure S12. Orbital interaction between LP of N1 and (a) BD* C5□O3, (b) BD* C2□C3, (c) BD* C1□C2, and (d) BD* C3□H4 for AMP-carbamate (LP: lone electron pair orbital, BD*: antibonding orbital).

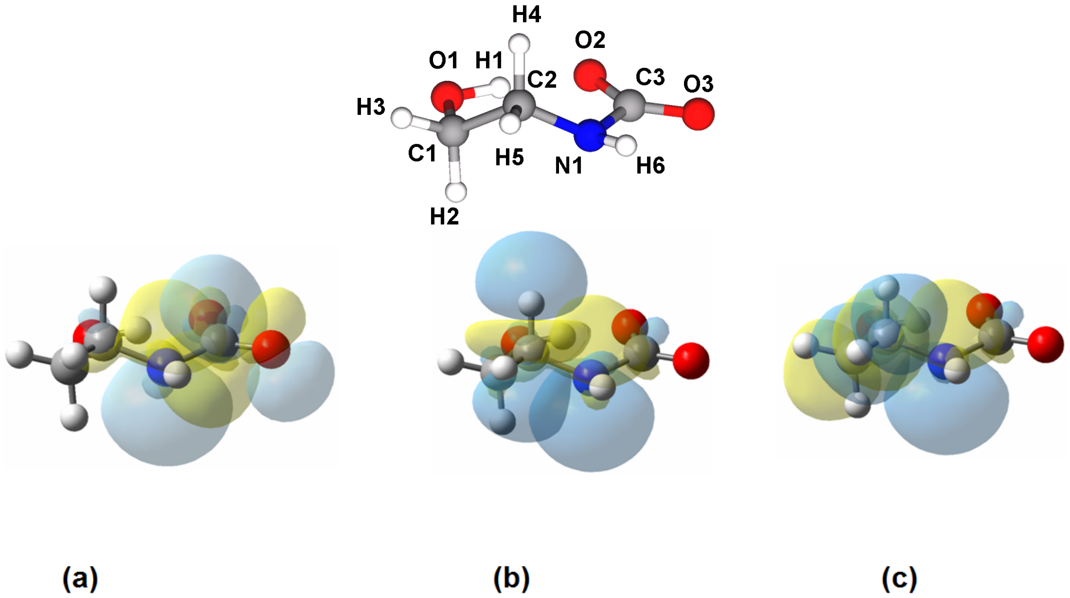

Figure S13. Orbital interaction between LP of N1 and (a) BD* C3□O3, (b) BD* C2□H4, and (c) BD* C1□C2 for MEA-carbamate.

Population analysis (NPA)

The charge distribution in carbamates are investigated using NPA population analysis (B3LYP/6-311++G(3df,3pd)) method.

Table S6. Population analysis using NPA for AMP- and MEA-carbamates.

AMP-carbamate	
Atom	charge (e)
C1	–0.02080
C2	0.08609
C3	–0.59588
C4	–0.57898
C5	0.94115
N1	–0.74352
O1	–0.83808
O2	–0.86013
O3	–0.85285
H1	0.49844
H2	0.15673
H3	0.17452
H4	0.20626
H5	0.20268
H6	0.20965
H7	0.21192
H8	0.20767
H9	0.20692
H10	0.38820

MEA-carbamate	
Atom	charge (e)
C1	-0.02827
C2	-0.21549
C3	0.93569
N1	-0.73719
O1	-0.84145
O2	-0.86510
O3	-0.85348
H1	0.49931
H2	0.14987
H3	0.17163
H6	0.39357
H4	0.17801
H5	0.21289